

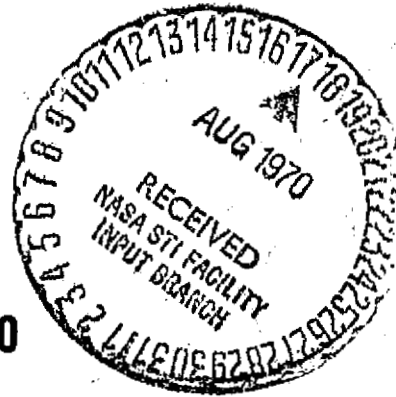
X-733-70-250

NASA TM X-63985

**ATMOSPHERIC EFFECTS ON
MILLIMETER WAVE
COMMUNICATION CHANNELS**

ERWIN MONDRE

MARCH 1970



GODDARD SPACE FLIGHT CENTER
GREENBELT, MARYLAND

FACILITY FORM 602

<u>N70-34446</u> (ACCESSION NUMBER)	_____ (THRU)
<u>45</u> (PAGES)	_____ (CODE)
<u>TMX-63985</u> (NASA CR OR TMX OR AD NUMBER)	<u>07</u> (CATEGORY)

X-733-70-250

ATMOSPHERIC EFFECTS ON MILLIMETER WAVE
COMMUNICATION CHANNELS

by

Erwin Mondre

March 1970

Goddard Space Flight Center

Greenbelt, Maryland

CONTENTS

	Page
ABSTRACT	v
INTRODUCTION.	1
WAVE PROPAGATION THROUGH THE ATMOSPHERE	3
General	3
Losses in Clear Atmosphere	5
Losses Due To Condensed Water	13
Fine-Grain Statistics for Rainfall	17
Refraction.	22
Scintillation.	23
Noise	25
CHANNEL CHARACTERIZATION	28
General	28
Black-Box Parameters	29
Channel Characterization Function	30
ATTENUATION MEASUREMENTS	33
Improvement by Path Diversity	37
References	40

PRECEDING PAGE BLANK NOT FILMED.

ABSTRACT

In order to meet future earth-to-space communication needs, new regions of the electromagnetic spectrum must be utilized. The feasibility of using the millimeter wave region will be discussed. One important factor is the attenuation under a variety of atmospheric conditions. High reliability can be achieved by the use of space diversity techniques to overcome the high attenuation due to heavy rainfall. Characterization and measurement of the performance parameters describing the communication channel are discussed.

PRECEDING PAGE BLANK NOT FILMED.

ATMOSPHERIC EFFECTS ON MILLIMETER WAVE
COMMUNICATION CHANNELS*

by

Erwin Mondre

Goddard Space Flight Center

INTRODUCTION

The history of radio communication has been characterized by a continuous push to higher and higher frequencies to make room for the increasing needs. The frequency bands currently used for earth-to-space communication are already allocated to terrestrial services, which produces certain interference problems. This frequency band between 1 and 10 GHz, commonly called our radio window, has indeed many advantages for communication both on terrestrial links and earth-space links. The tropospheric and ionospheric effects are very low in this range, but this region of the electromagnetic spectrum is already overcrowded.

Taking into account the estimated increase in both telephony and television in the United States, the presently used 4- and 6-GHz bands will be exhausted by 1980. These estimates already include multiple-beam systems and optimal

*This work was accomplished while the author held a National Research Council Postdoctoral Resident Research Associateship supported by the National Aeronautics and Space Administration.

separation in a satellite communication network. Not included in these estimates are the expected data transmissions between machines and machines, and from machines to people. Also, the exploration of outer space will require high data rate transmission channels.

For many years the potential applications of millimeter waves for communications have been known; yet for many years this region of the spectrum has been essentially neglected. In fact, with the advent of the laser, there was a temporary lull in millimeter wave research and it was suggested that millimeter waves may have passed from infancy to obsolescence. However, recent progress in millimeter waves indicates they are just reaching maturity. The event that is most responsible for the progress in millimeter waves is the space age. In the space age many new applications for millimeter waves are found, and these in turn produce a requirement for new and improved components.

The amount of information that can be transmitted in a given time is proportional to the bandwidth that is available. There are certain factors that restrict the bandwidth. First is the state of the art of components for a particular frequency band. The rapid progress in the art of solid-state devices has made it certain that technology alone will not be the ultimate factor limiting or excluding the availability of almost any frequency band. Moreover, the hardware is not the topic of this paper; therefore, this factor is ignored. The second important factor that restricts the availability of the bandwidth is the nature of the propagation medium in which the communication channel is situated. For

communications, and especially for space communication, the media are the atmosphere (troposphere and ionosphere) and the interplanetary space. The latter has little effect on propagation, even at lower frequencies. The ionosphere, a weakly ionized medium extending from about 50 to 1000 km above the surface of the earth, can distort a signal passing through it at lower frequencies. The effect becomes less for the L- and the lower portion of the S-band. Ionospheric effects have not placed significant limitations on communication at microwave frequencies (S-band and above). There should be no measurable effect on millimeter waves.

WAVE PROPAGATION THROUGH THE ATMOSPHERE

General

The troposphere is the lower portion of the earth's atmosphere and extends from the surface of the earth to about 20 km. It is by far the most important portion to consider. There is an electromagnetic "window in space" at the frequency (or wavelength) at which one-way attenuation through the atmosphere is less than one-half, or 3 dB (Figure 1). * The frequency range shown goes from microwave to ultraviolet. Although the average transparency of the atmosphere is not high, the total bandwidth still available is enormous. Between 10^{10} and 10^{15} Hz, there is a total of 7.8×10^{14} Hz available. The major part is in the right-hand corner—the optical frequency region—due to the logarithmic scale. For example, one could transmit 10^7 television bands of 72 MHz. Looking only at the millimeter wave

*Kompfner, R., "Windows to Space (From 10^{10} Hz Up)," 13th AAS Meeting, Dallas, Texas, May 1-3, 1967.

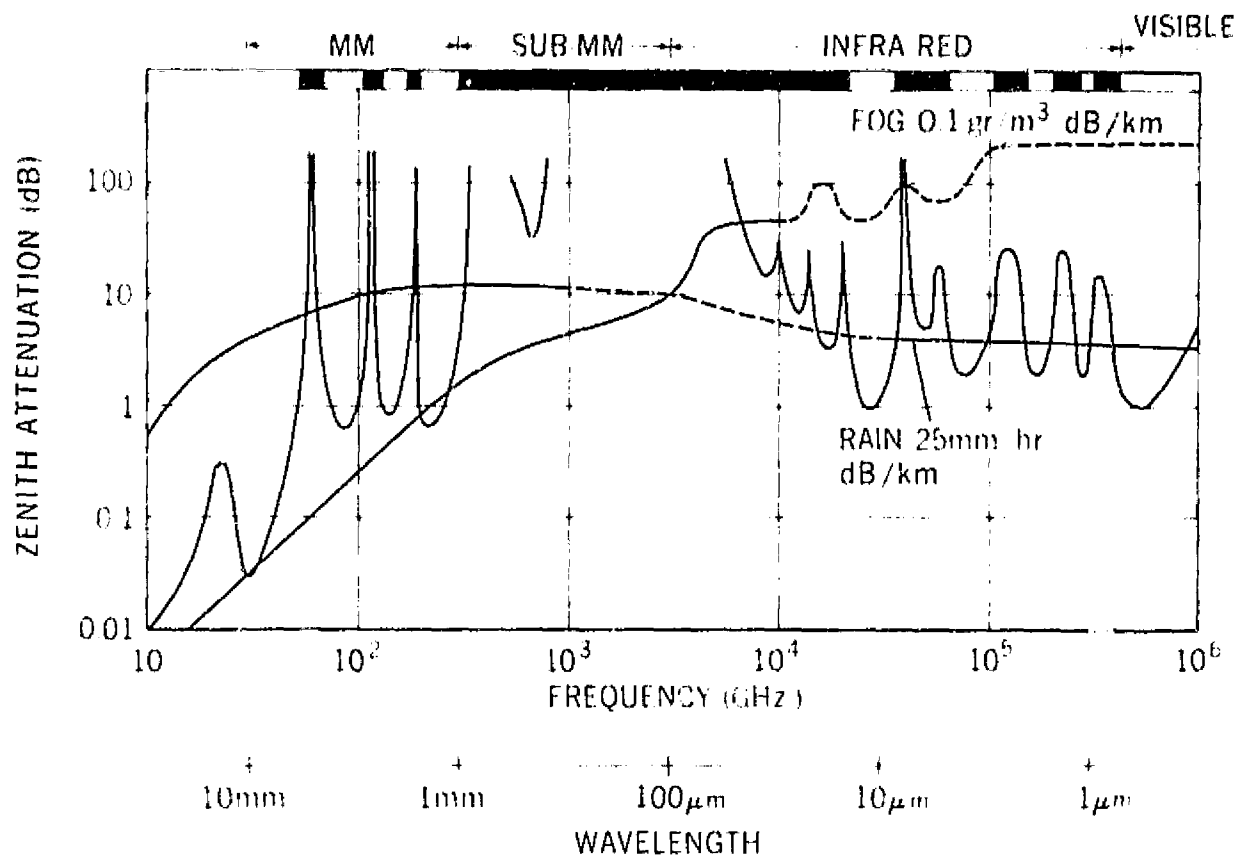


Figure 1—Windows in the atmosphere.

region from 10 to 320 GHz, the total window bandwidth is still 200 GHz, or 3000 times the 72 MHz television band. Also shown in Figure 1 is the attenuation (in dB/km) versus frequency for fog and rain. One can see that it is the rain that makes communication difficult at millimeter wavelengths; whereas at laser frequencies fog is more serious. This will be discussed in detail later. Since the troposphere is the most important part of the medium between transmitter and receiver, one must look at the chief components, which are gases such as nitrogen, oxygen, argon, water vapor, and carbon dioxide, and various kinds of precipitation.

How do the combined physical properties of these components affect the communication channel? To obtain a clear picture it is convenient to consider the different physical effects separately. First, look at the clear and idealized atmosphere where there are the electromagnetic windows. Next, consider the effects of condensed water, then, the effects of atmospheric inhomogeneities, and finally, consider the interference (noise) produced by atmosphere, sun, and planets.

Losses in Clear Atmosphere

The physical cause of the attenuation over most of the frequency range is molecular absorption. Electromagnetic energy is turned into heat. The earth's atmosphere emits and absorbs electromagnetic radiation of all wavelengths. The magnitude of the emission and absorption, however, is not significant at wavelengths longer than 3 cm, except for long transmission paths parallel to the earth's surface. Some of the atmospheric gases causing emission and absorption in the millimeter wave region (Reference 1) are shown in Figure 2. The line resonance frequencies are shown for O₂, H₂O, O₃, CO, SO₂, N₂O, and NO₂.

At millimeter and submillimeter wavelengths, oxygen and water vapor are the primary sources of emission and absorption in the atmosphere. Nitrogen, which has neither electric nor magnetic moments, does not emit or absorb. Although they have large values of peak attenuation at millimeter wavelengths, other atmospheric gases, such as ozone, hydrogen, sulfide, and carbon monoxide, produce negligible attenuation because of their low molecular densities.

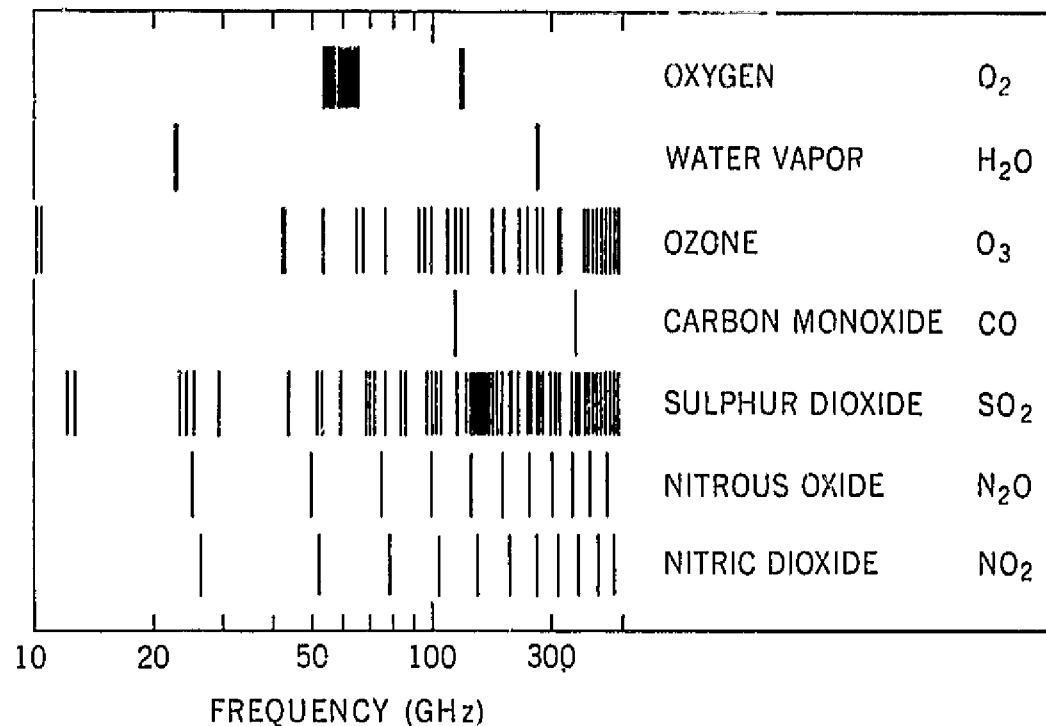


Figure 2—Line frequencies of several atmospheric gases.

Resonance lines for water vapor and oxygen for the standard atmosphere (temperature of 293°K , pressure of 760 mm Hg, and 7.5-g/m^3 water vapor concentration) are shown in Figure 3. As already pointed out, the absorption peaks are produced by energy transition in the molecules. It can be seen that most of the energy transition results in peak values of absorption at the sub-millimeter and infrared region of the electromagnetic spectrum. The interaction of electromagnetic radiation with water vapor is associated with the electric dipole moments of the water molecule. In O_2 , which is paramagnetic, the magnetic moments are responsible for absorption. The curve (Figure 3) is calculated from the Van Vleck and Weisskopf equation. In the submillimeter region are 871 absorption lines. The attenuation reaches peak values of 10^4 to 10^5 dB/km. The maximum absorption in the windows is found in the region of 1000 to 10,000 GHz. Actually, they should not be called windows; they are

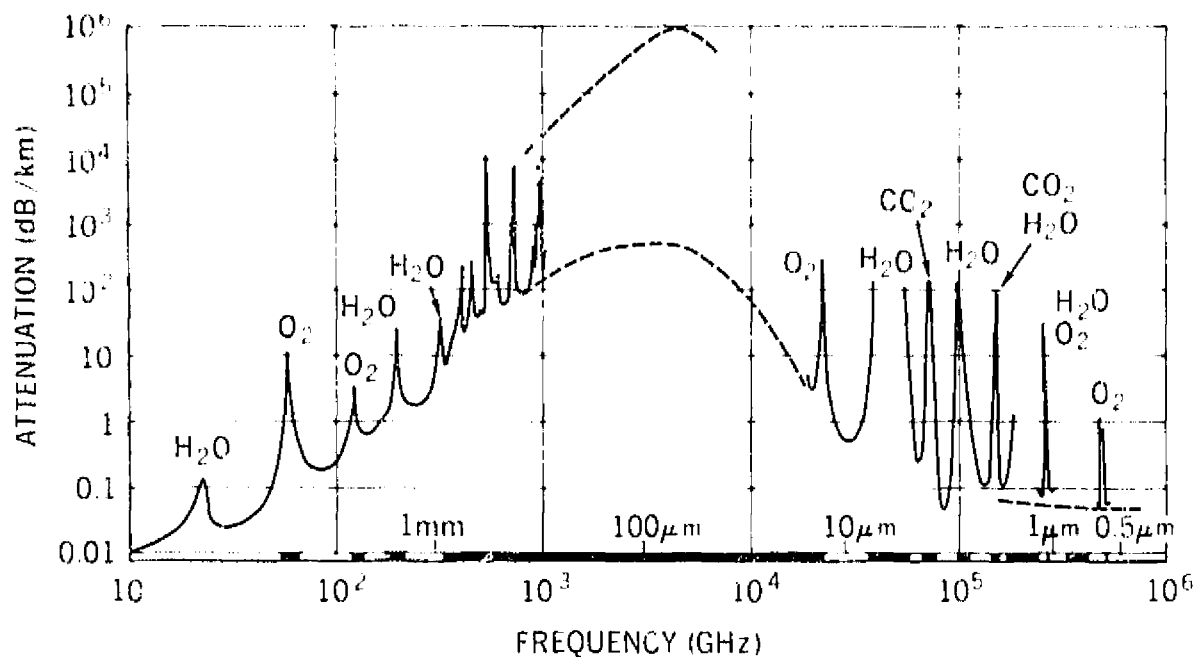


Figure 3—Atmospheric attenuation.

regions of high attenuation enclosed by peaks of even higher attenuation. The absolute value of absorption decreases sharply with increase or decrease in frequency.

Now, take a closer look at the millimeter wave region illustrated in Figure 4. Between 10 and 300 GHz there are 2 water vapor lines, which are located at 22.235 and 184.4 GHz. For a standard atmosphere at sea level the peak attenuation at these lines is 0.2 and 30 dB/km, respectively. The 22-GHz line produces no restriction since the attenuation is very low. There are also two very strong O₂ absorption lines in the millimeter wave region. One is near 60 GHz (this line consists actually of many closely spaced lines), and the other single line is at 119 GHz. The peak absorption at these two lines is 13 dB/km and less than 2 dB/km, respectively. The absorption lines are not exactly lines; they are not concentrated at a single frequency but show a rather wide spread over a frequency

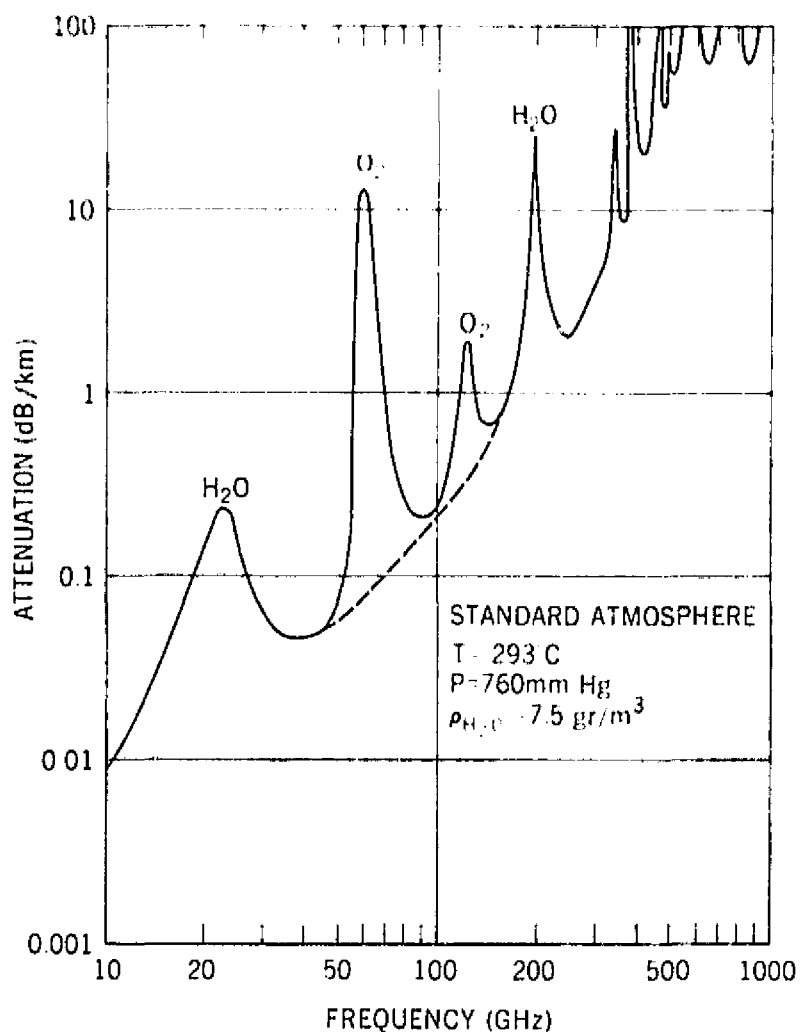


Figure 4—Attenuation at sea level.

interval. The reason for this line broadening is the atmospheric pressure. Therefore, this is often referred to as pressure broadening. The slopes of the H₂O resonance curves are dependent on atmospheric temperature, pressure, and partial pressure of H₂O; whereas the slopes of the O₂ lines are functions of atmospheric temperature and pressure.

The discussion has been about the attenuation derived from a theoretical model. There is a good agreement between measured data and the theoretical curve, provided suitable values are taken for the pressure-broadening constants — namely, the frequency widths. The O₂ and H₂O lines have been measured

(Reference 2) and are shown in Figure 5. The experimental data were obtained from measurements carried out at the University of Texas (T), Bell Telephone Laboratories (B), and the Aerospace Corporation (A). This plot shows again the attenuation (in dB/km) for sea level atmosphere and a water vapor content of 7.5 g/m^3 .

As already pointed out, the atmospheric attenuation depends on temperature and pressure. Therefore, there is a very rapid decrease in attenuation per kilometer with increasing height. For an earth-to-space link one has to take into account the attenuation through the entire earth's atmosphere (Figure 6). These curves can be determined by interpolating the values of the attenuation to all elevations of the earth's atmosphere. These values can also be derived from temperature and pressure profiles and from integration of the Van Vleck and Weisskopf equation. Commonly accepted models of height variations of the molecular density, absolute pressure, and temperature are used to calculate the attenuation (Reference 3). Each band of frequencies, each window, has distinctive propagation characteristics. In general, however, increasing the elevation of a groundbased terminal will decrease the attenuation of the atmosphere simply because of the decrease in water vapor and oxygen density with increased elevation.

The total atmospheric attenuation, which is relatively low at angles near zenith, increases with decreasing elevation angle and becomes very large near the horizon (Figure 6). The amount of the lower atmosphere traversed ranges

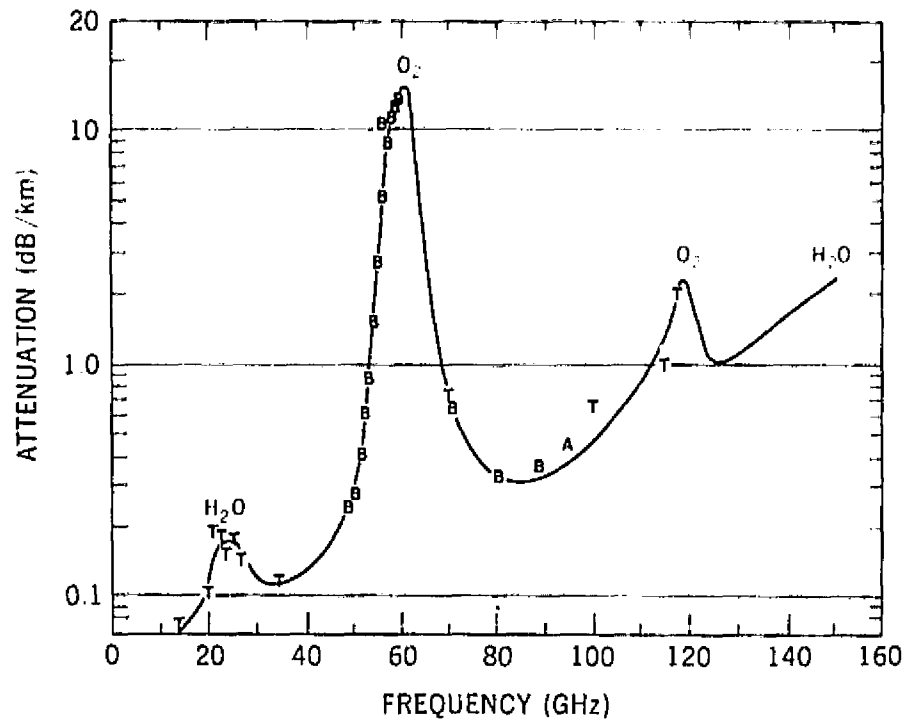


Figure 5—Attenuation in clear atmosphere.

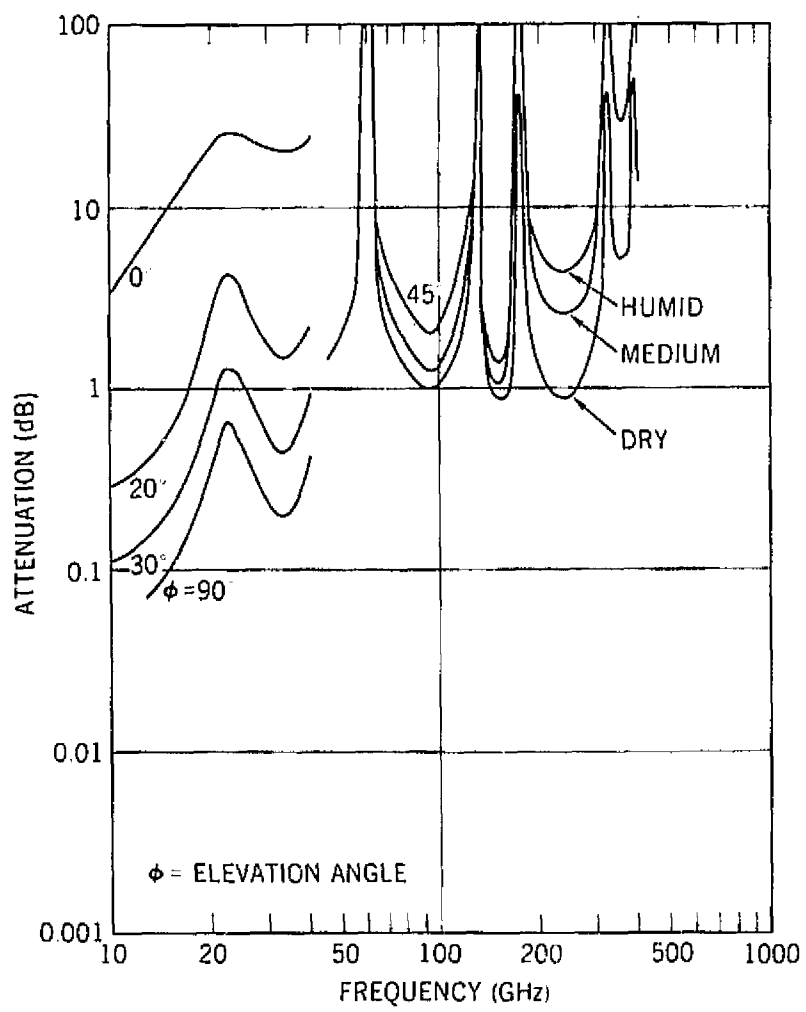


Figure 6—Total attenuation for one-way transmission through the atmosphere.

from 20 km near zenith to about 500 km along the horizon; for this reason, it becomes quite apparent why attenuation at angles near the horizon is so large. Note that there are large bands of wavelengths throughout the spectrum where the vertical and near-vertical attenuation is relatively small. It is also interesting that, for standard atmosphere and frequency of 32 GHz for example, the attenuation for a zenith-oriented signal is roughly the same as the attenuation for a signal traversing a 2-km path along the earth's surface. Therein lies the advantage in using these frequency bands for satellite communication. Propagation through the atmosphere occurs only twice when satellite relay stations are used.

Now consider the 60-GHz oxygen absorption lines. The attenuation (in dB/km) versus frequency for a horizontal path at different elevations for the 60-GHz region is shown in Figure 7. At sea level the individual lines overlap, due to pressure broadening, and form a continuous region of high absorption. The attenuation is above 3 dB/km from 55 to 65 GHz. At higher altitudes the attenuation becomes smaller due to the decrease in atmospheric pressure, and the individual lines can be seen. There are 25 closely spaced resonance lines which have been calculated and observed (Reference 4).

The vertical attenuation through the entire standard, tropic, and arctic atmospheres in the 60-GHz region is shown in Figure 8 (Reference 1). The lower curve is the attenuation from an altitude of 10 km into space. This elevation represents the commercial airline altitude. Even here the attenuation is above

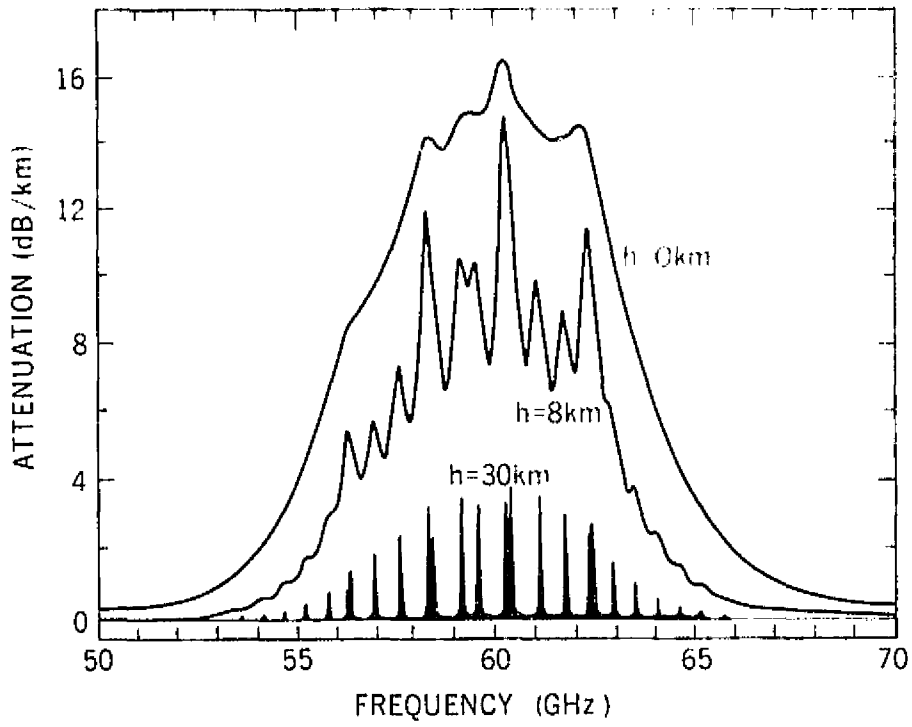


Figure 7—Oxygen lines at 60 GHz.

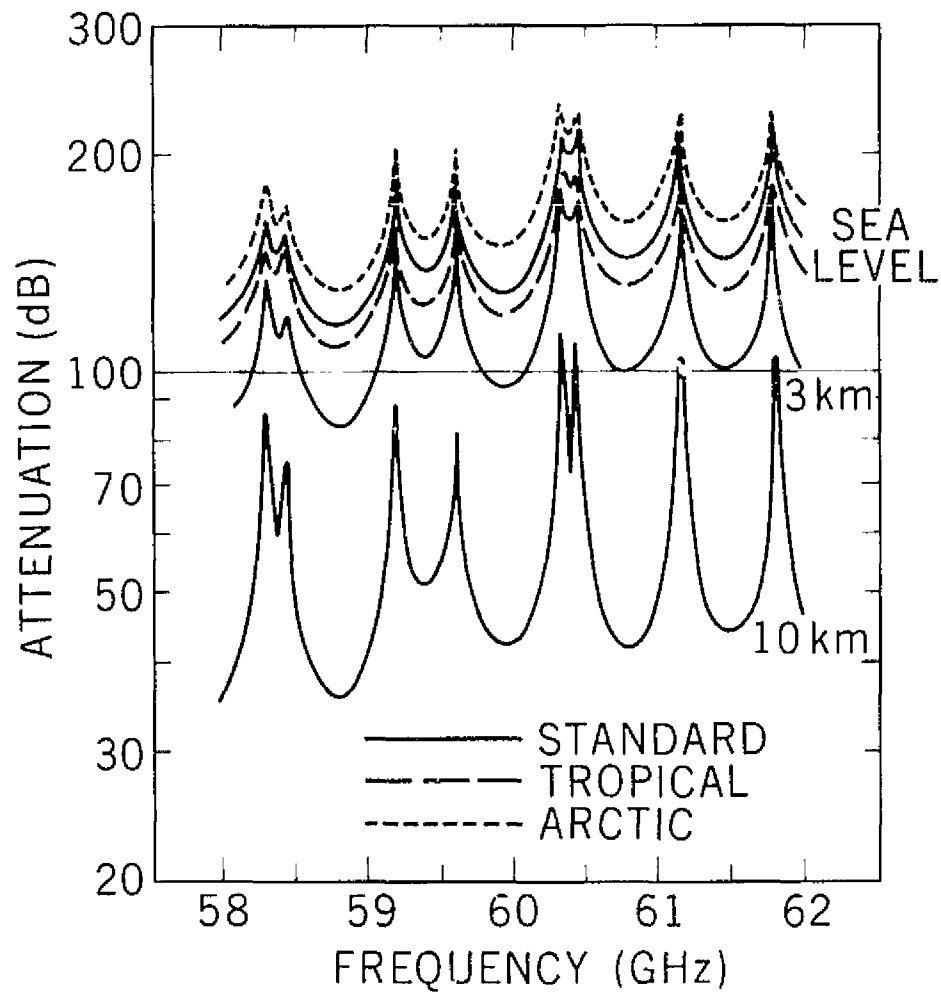


Figure 8—Attenuation through standard, tropic, and arctic atmospheres.

40 dB, which suggests the use of this frequency band for secure and interference-free communication between satellites and/or highflying aircraft. The very complex resonance structure around 60 GHz can be used for scientific radiometric measurements of the earth's atmosphere. Temperature, oxygen density, and magnetic field strength (detectable due to the Zeeman splitting) can be determined.

Losses Due To Condensed Water

Another constituent of the atmosphere that contributes to the losses is precipitation. The attenuation due to condensed water for different frequencies is listed in Table 1. Here, "very severe" attenuation means that the loss may be of the order of 100 dB; "severe" is several tens of dB, "moderate" may be 10 dB or so, and "light," a few dB. One can see that, of all forms of precipitation, rain has the most serious effect on millimeter wave propagation. Although the basic features of attenuation of millimeter waves by rainfall are known, some details are not. When a microwave impinges upon a drop of water, part of it is absorbed and dissipated as heat and the remainder is scattered. At centimeter wavelengths, absorption is predominant because the drop sizes of rain are small compared to the wavelengths. Thus, the attenuation is roughly proportional to the liquid water content.

However, millimeter wavelengths are of the same order as the diameter of the larger raindrops, and this complicates the behavior of the attenuation as a function of frequency. Nevertheless, the problem has been solved exactly for drops of arbitrary size with given dielectric and loss coefficients. The theory

Table 1 — Qualitative appraisal of one-way attenuation for radiation through the atmosphere.

Precipitation		Frequency Range			
Type of Condensation	Approximate Droplet Size	10^9 to 10^{11} (mm waves)	$3 \cdot 10^{13}$ (10-cm window)	10^{14} (3, 5-cm window)	$3 \cdot 10^{14}$ to 10^{15} Hz (visible light)
Heavy rain	5 mm	Moderate to severe	Moderate to severe	Moderate to severe	Moderate
Light rain	0.1 to 2 mm	Light to moderate	Light	Light	Light
Sea mist	10 to 100 μ m	Light	Moderate	Moderate	Moderate to severe
Heavy fog	0.1 to 10 μ m	Light	Severe	Severe	Very severe
Clouds and fog	1 to 10 μ m	Negligible	Moderate to severe	Moderate to severe	Severe
Light haze	0.1 to 1 μ m	Negligible	Negligible	Light	Light to moderate
Snow	Crystals of various sizes	Negligible	Severe	Severe	Severe

was derived by Mie and treats spherical particles of any material in a nonabsorbing medium. It takes into account both absorption and scattering. It has been found that attenuation due to rain is approximately proportional to the number of droplets per unit volume.

It is evident from the theory that the maximum and minimum possible attenuation will result when the rain is composed of drops of the same size (Figure 9). The attenuation, in these cases, is proportional to the rainfall rate (Reference 5). The discontinuities of the slope in the lower curve at 30 GHz and upper curve at 5 GHz occur because in these regions the drop size for maximum and minimum attenuation jumps from one end of the range of diameters to the other. Also shown in this plot is the attenuation assuming the Laws and Parsons drop-size distribution.

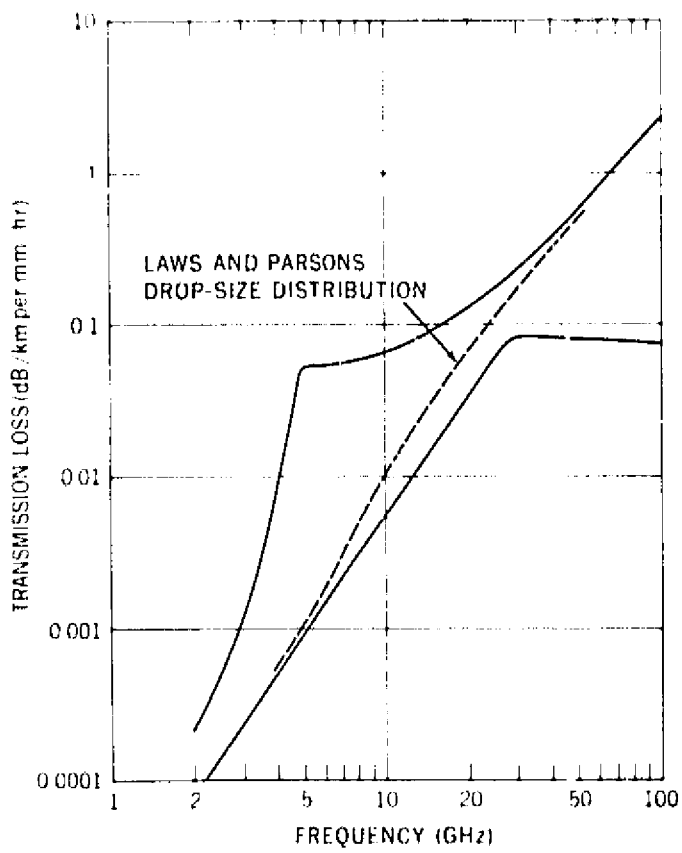


Figure 9—Theoretical maximum and minimum attenuation due to rainfall (uniform drop size).

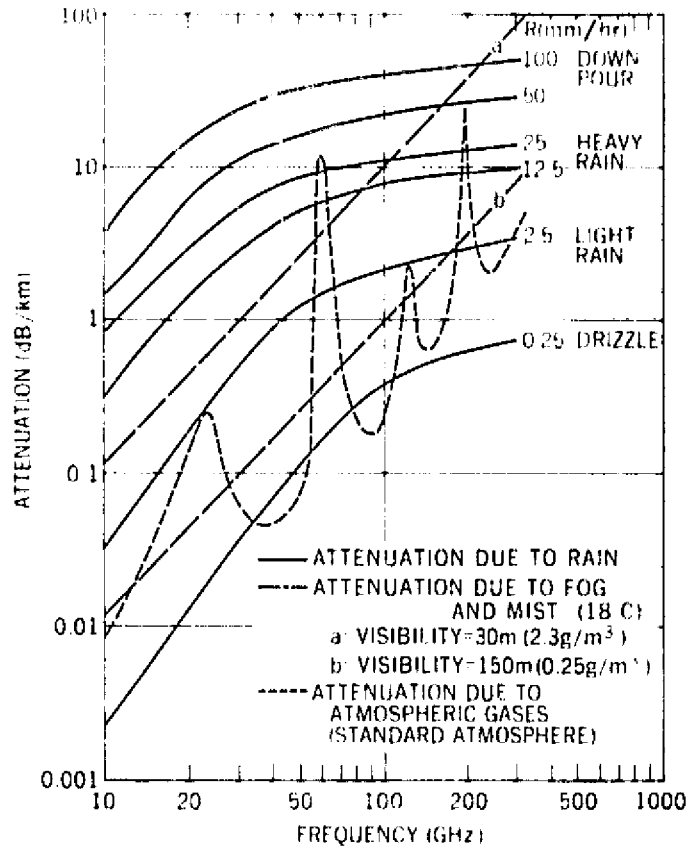


Figure 10—Attenuation due to rain and fog.

A combination of the theoretical attenuation and experimental drop size distribution for a given rainfall rate yielded the plots shown in Figure 10. The increased attenuation at millimeter wavelengths is due to the increased size of the particles relative to the wavelength. The most significant loss results from scattering of the energy by particles with diameters in excess of one-tenth of a wavelength. The temperature influence in the range of 10° to 30°C and for wavelengths less than 3 cm is not to exceed $\pm 20\%$, but no clear trend can be shown. In general the influence is much less. Besides, this is considerably less than some of the discrepancies between the theoretical and measured values.

Most of the experimental data show that the measured attenuation is above the maximum value predicted by the theory. Thus, the applicability of the Mie

theory to the practical rainfall situation cannot be said to be demonstrated. In view of this, and also of the very large scatter in the measured points that is often observed, the attenuation curves obtained by applying the Mie theory to the Laws and Parsons drop-size distribution can only be taken as giving a rather crude estimate. An improved theory predicts that at a particular frequency the attenuation will not be strictly proportional to the rainfall rate; the reason for this is the variation in drop-size distribution with rainfall rate. The drop-size distribution near the earth's surface is known with considerable confidence. Its form depends on the rainfall rate and, to some extent, on location. What are the reasons for the discrepancy? Why is the measured attenuation usually 1.5 to 2 times as high as the predicted value?

There are at least three types of experimental errors:

(1) Uncertainty in measuring the effect of the wind can produce errors since it is to be expected that in the presence of wind, and gusty wind particularly, the water density in the air will be subject to variations even though the rainfall rate on the ground appears unchanged.

(2) The number of rain gauges is usually quite inadequate to ensure that measurements be made only under conditions of uniform precipitation along the path.

(3) The presence of fog and mist introduces differences, but this effect should be negligible for rainfall rates of 50 mm/hr or more.

On the other hand, the theory neglects multipath scattering effects along the path. Rain structure may also be more complex than assumed; rain may tend to contain clusters of two or more closely spaced drops.

Consider now the attenuation due to other forms of precipitations and clouds. Attenuation due to clouds occurs through both absorption and scattering. Cloud droplets are generally less than 100 μm in diameter, therefore, even at millimeter wavelengths the Rayleigh approximation (diameter \ll wavelength) holds. It is found that attenuation from water clouds is much larger than that from ice clouds and that, for both cases, the losses are due mainly to absorption rather than scattering. It has been shown that the attenuation depends more on total liquid water content than on droplet-size distribution. Hail and dry snow have negligible absorption in the millimeter wave region. Wet snow, on the other hand, has been shown to attenuate more strongly than water spheres of the same volume. Mist and fog, similar to clouds, also attenuate the electromagnetic radiation (Figure 10). The attenuation is proportional to water content and increases linearly with frequency (Rayleigh approximation). However, the attenuation is also affected by temperature, and reduction to 0°C will cause the attenuation to be nearly doubled for frequencies below 30 GHz.

Fine-Grain Statistics for Rainfall

Rainfall rate has been measured with gauges which collect water and indicate that a given amount has fallen. Such devices measure average rainfall over a considerable period. If we wish to evaluate the reliability of a communication

system on the basis of rainfall data, those data must be resolved in time down to minutes and seconds per year. High-speed rain gauges with instantaneous reading (high time resolution) have been developed (Reference 2). A readout made on such a gauge is shown in Figure 11. This record was taken during a brief, intense summer shower in New Jersey. Within seconds, the rain rate at a given point changed by a factor as great as 10. Long term statistics obtained with such devices are necessary for the design of millimeter wave radio systems.

Another method of obtaining highly resolved rain rates is that of photographing, counting, and measuring the drops in a given volume of rain. Data obtained by this method (from Illinois State Weather Survey, 1-year study), reduced to percentage-of-time distribution of rainfall rate are presented (Figure 12). Note that the measurements extend to 0.0001 percent of the time, which is about 30 seconds per year. Perhaps it is not surprising that heavy showers in Miami have maximum rain rates about 20 times greater than those of heavy showers in Ottawa. However, it is surprising that, for a short time, the point rainfall rate (the rate at a given point) in Miami can exceed 700 mm/hr. The distribution from Bedford (England) and Ottawa were obtained by other methods (1-km spacing of gauges and 2-min average reading).

This discussion has been centered on the temporal rather than the spatial rainfall structure. However, it is known from our everyday experience and from dense rain-gauge networks that storms, heavy showers particularly, have rather fine-grain spatial characteristics. How fine-grained these characteristics

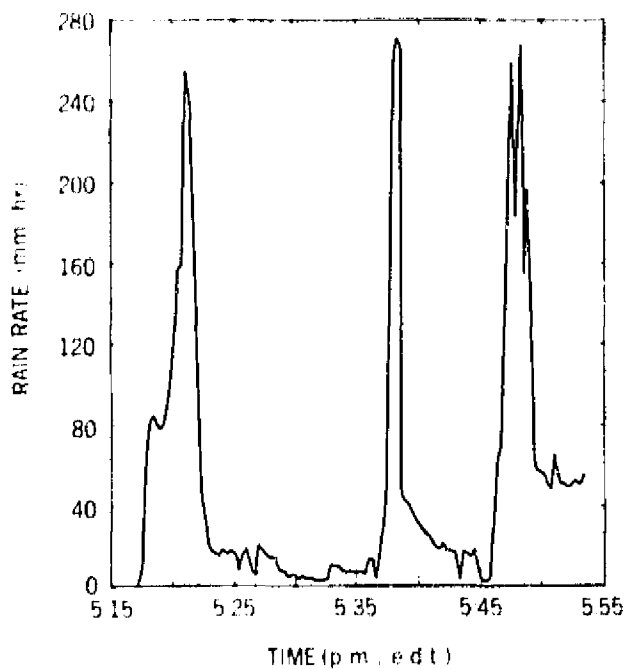


Figure 11—Rain rate measured at one location (Holmdel, N.J.) as a function of time.

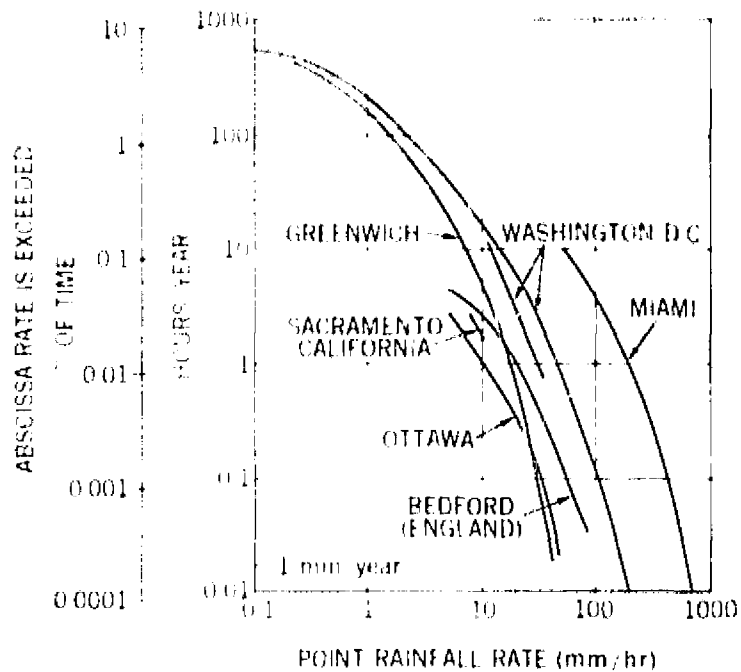
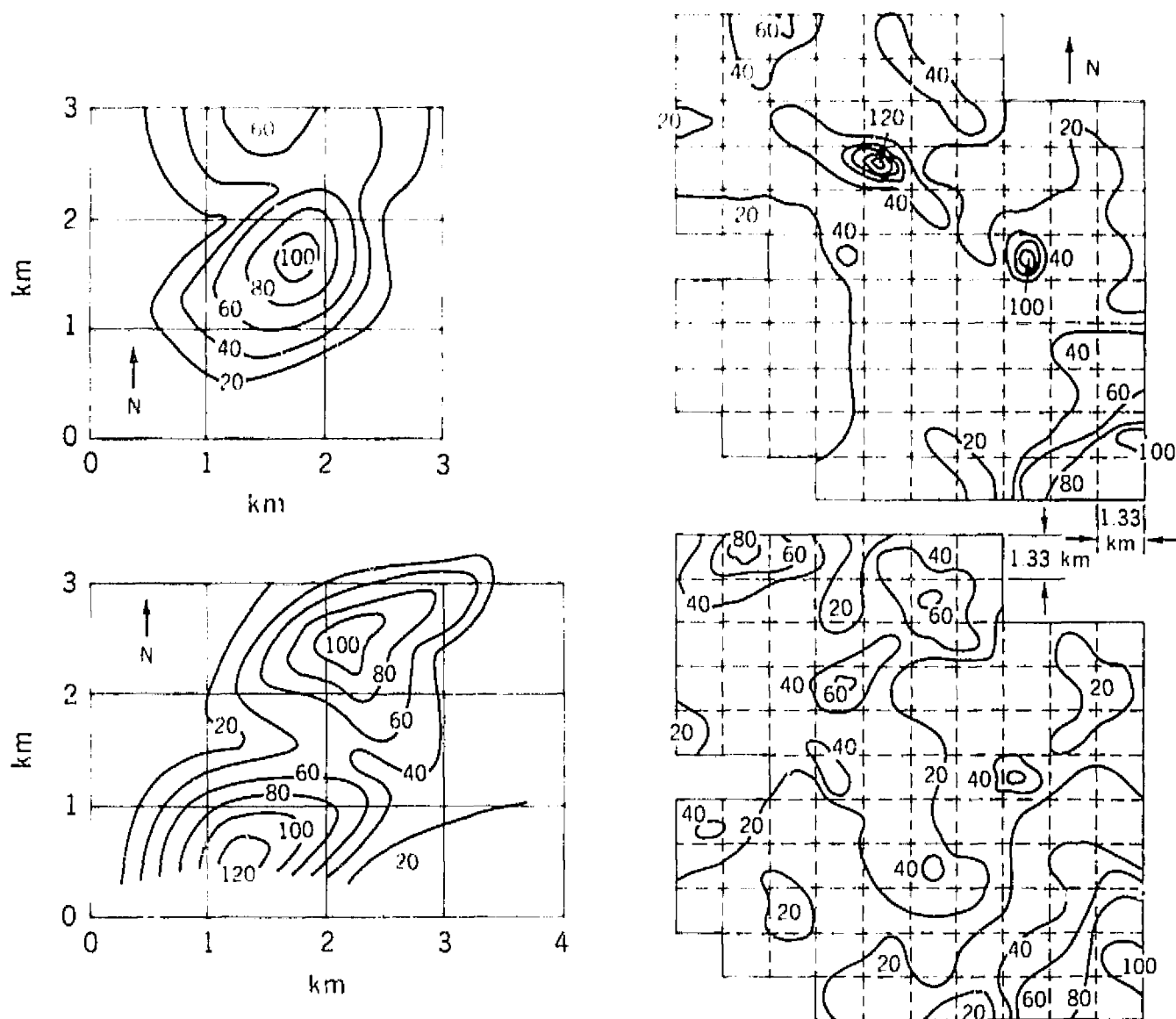


Figure 12—Yearly rainfall distribution.

of heavy showers are still a matter for research. Spatial structure can be demonstrated by examples of data taken on two rain-gauge networks of rather high resolution, one in Bedford, the other in New Jersey (taken from Reference 2).

The Bedford network covers an area of about 3 km^2 and has an intergauge spacing of about 1 km. The readings of rainfall rate for the system at a chosen instant can be linearly interpolated between a given gauge and its nearest neighbors. In this way a contour map can be plotted. The result of such a procedure is shown in Figure 13a. On top, there is evidence of two rather discrete cells. The lower part shows conditions 2 min later. The two cells have moved about 1 km toward the south during the 2-min interval. This movement is equivalent to a translational velocity of about 32 km/hr. The details of the rain structure are fairly clear in the lower plot. However, because there is only one gauge per square kilometer it is not certain that the maximum rates given at the centers



a-(top) Plot of rainfall-rate contours (mm per hr), showing two rain cells on the Bedfordshire rain-gauge network; (bottom) contours 2 min later.

b-(top) Plot of rainfall-rate contours (mm per hr) showing several rain cells on the Holmdel, New Jersey rain-gauge network; (bottom) contours 10 sec later.

Figure 13-Rainfall-rate contours.

of the cells are the actual maximum rates. That is to say, the true centers of the cells may not have passed over the points where the gauges are located. As for the shape and size of the cells, it is not known that linear interpolation between gauges is an optimum procedure for determining this.

The New Jersey network covers an area about 13 km^2 and has an intergauge spacing of 1.3 km. It consists of 96 rain gauges of the high-resolution type.

Because of the fast response of such gauges, contour maps can represent conditions separated by an interval of as little as 10 sec, as shown in Figure 13b. On top, there is evidence of four fairly discrete cells; the most intense of these is located in the upper portion and has a maximum rainfall rate of 120 mm/hr. Conditions 10 sec later are shown below. The intensity of the cell in the upper central section has decreased to 60 mm/hr in this short interval, and a similar decrease in intensity has occurred in the central-eastern section. Apparently this figure represents two different types of rainfall dynamics. The intensity of the cell is well preserved over the 2-min interval, and the cells appear merely to undergo a translation. But the position of the two central cells appears to be stationary whereas their intensity decreases significantly during the 10-sec interval. This represents the "on-off" character of the rainfall intensity.

In calculating attenuation for earthbased radio-relay systems, one is interested not in point rainfall rates *per se*, but rather in the average rate along a particular propagation path. If one tries to use only point rainfall data in designing a system he must ask whether there is any relationship between point- and space-averaged rainfall rates. Provided certain restrictions (not yet fully defined) are placed on the length of path over which the average is taken, such space-time relation is valid (Reference 6).

For a ground link, the attenuation due to rain can be estimated with certain accuracy if the measurement effort on the ground is increased. Unfortunately, this is not the case for a space link. In the evaluation of the use of millimeter waves for space communication, what is needed is a set of attenuation distribu-

tions for a propagation path extending through the atmosphere at a fairly high elevation angle rather than along the surface of the earth. No such experimental distributions exist. Nor is it possible to calculate with any certainty what these attenuations would be, because the liquid water content and the distributions of drop size are unknown for such nearly vertical paths. Also there is always a great uncertainty in the length of the path influenced by rain, since the top level of the rain-bearing clouds cannot be defined accurately. Therefore, it will be necessary to measure the attenuation directly, without trying to estimate these values from measured ground rainfall rates. The methods that can be used to measure the attenuation will be discussed later.

Refraction

Attenuation of millimeter wave signals due to atmospheric gases (molecular absorption) and due to condensed water (absorption and scattering) has been discussed. In addition, refraction also introduces losses to a millimeter wave signal. Attenuation due to refractive losses should be distinguished from attenuation by absorption or multiple scattering since in the latter case the energy is, for all practical purposes, lost, but in the former case the wave is only bent, thereby resulting in a change in the angle of arrival at the antenna, which can be compensated for, if known.

An electromagnetic wave passing from one medium to another undergoes a change in velocity and, if it enters the second medium, generally experiences a bending called refraction. For a standard atmosphere a wave passing from the lower to the upper layer is bent downward. Under these conditions the apparent

position of a source outside the atmosphere appears at an elevation angle slightly greater than that corresponding to the true position. * The refraction correction for a standard atmosphere is shown in Figure 14 as a function of elevation angle for both millimeter waves and optical frequencies. For the dry atmosphere the index of refraction is essentially constant for the entire electromagnetic spectrum. The higher values of attenuation at millimeter wavelengths do not significantly change the refractive index of the atmosphere. When water vapor is added, it can be shown that the dipole moment of the molecule tends to follow electric field changes at millimeter wave frequencies but not at optical frequencies, and as a result the millimeter wave index of refraction is greater. Refractive effects vary widely with meteorological conditions and for some abnormal cases the wave bends sharply downward (super-refraction), upward (subrefraction), or becomes trapped (ducting).

At elevation angles near 90° the refraction error is negligible. Even at 50° elevation the error is less than 0.01° . At low elevation angles the refraction error is very large, but also the absorption is very large, prohibiting propagation at these low angles.

Scintillation

One of the characteristics of the millimeter wavelengths is the fluctuation of the signal associated with line-of-sight propagation. This scintillation is caused by variations in refraction and absorption. The effect is much like the

* Altshuler, E. E., "Earth-to-Space Communication at Millimeter Wavelengths," Physical Science Research Paper 125, Aug. 1965.

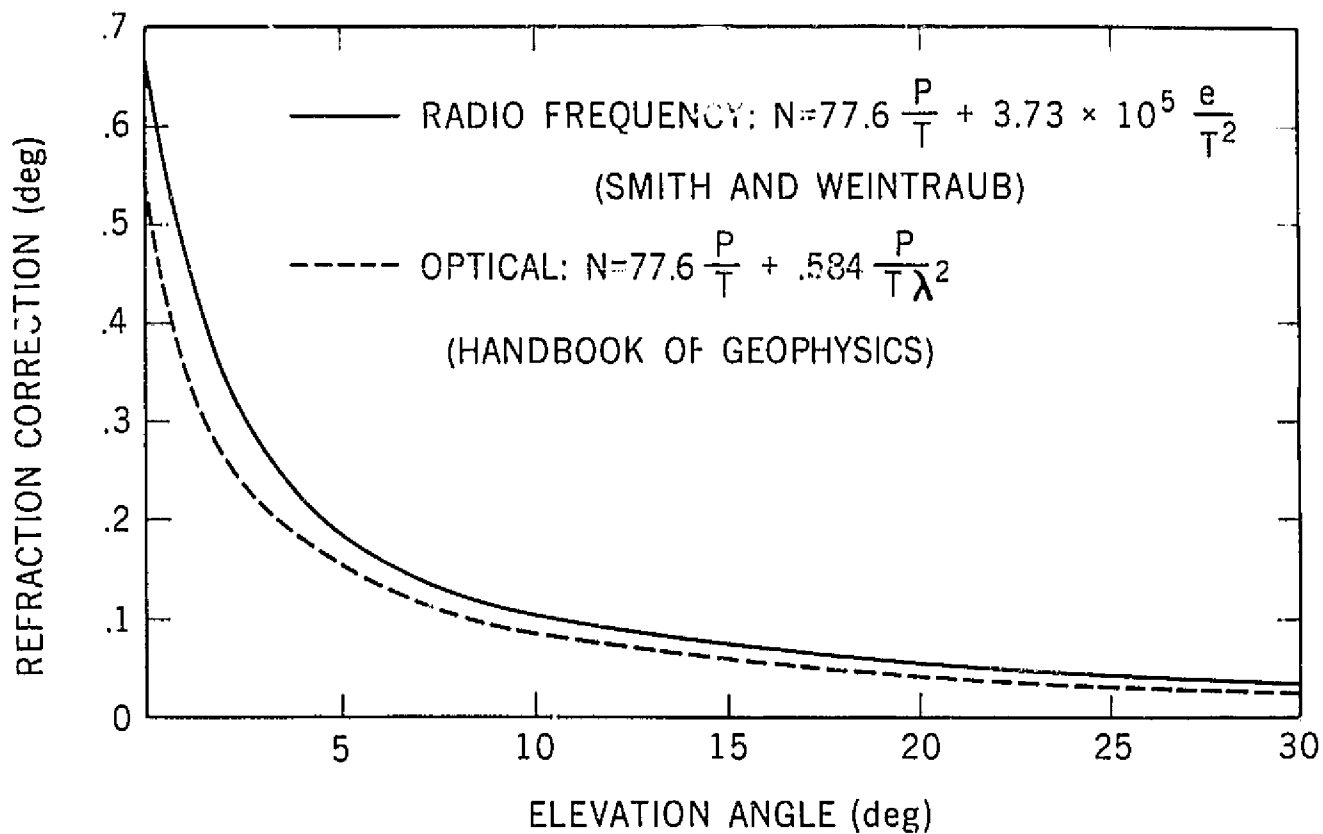


Figure 14—Refraction correction versus elevation angle.

twinkling of lights or stars at visible wavelengths. However, the magnitude of the scintillation at millimeter wavelengths is small compared with that of an optical system. Signal strength fluctuations are closely correlated with refractive index fluctuation. These fluctuations will, in general, decrease with elevation since refractive index fluctuations decrease rapidly with elevation above the earth's surface.

The ever-present refractive index fluctuations in the atmosphere could have two harmful effects on transmission of broadband information. One is that the phase front of the wave reaching a receiver would be so distorted that the receiving antenna, which is designed to accept a uniform phase front, would not function efficiently. This would cause an apparent decrease in antenna gain and an apparent broadening of the antenna beam. However, in transmission on the

earth and in radio-astronomy measurements in which large narrowbeam antennas are utilized, no significant beam broadening has been observed. The second effect associated with scintillation would be that of limiting the usable signal bandwidth because of time delays introduced by scattering from the refractive-index variations in the air. This effect is closely related to the beam broadening, since both are produced by the same mechanism.

Most of the measurements made of refraction and signal-level fluctuations through the atmosphere have been made with relatively narrow bandwidths (less than 10 Hz). One of the unanswered questions in this area, therefore, is the degree of restriction of information bandwidths that can be caused by the atmosphere.

Noise

The maximum data rate that can be transmitted over a given communication channel is, according to Shannon's formula, a function of bandwidth and signal-to-noise ratio. The limitations introduced by bandwidth and attenuation, that is, available signal strength at the receiver end of the channel, have been discussed. Now, consider the noise contributions at millimeter wavelengths. The total noise level of the overall system is a function of the noise figure of the receiver and the sky noise (antenna noise). A plotting of the sky temperature as a function of frequency, as observed and reported by various observers is shown in Figure 15. Strong noise sources, such as the sun, may contribute considerably to the background noise even if received through the sidelobes of the antenna. In the

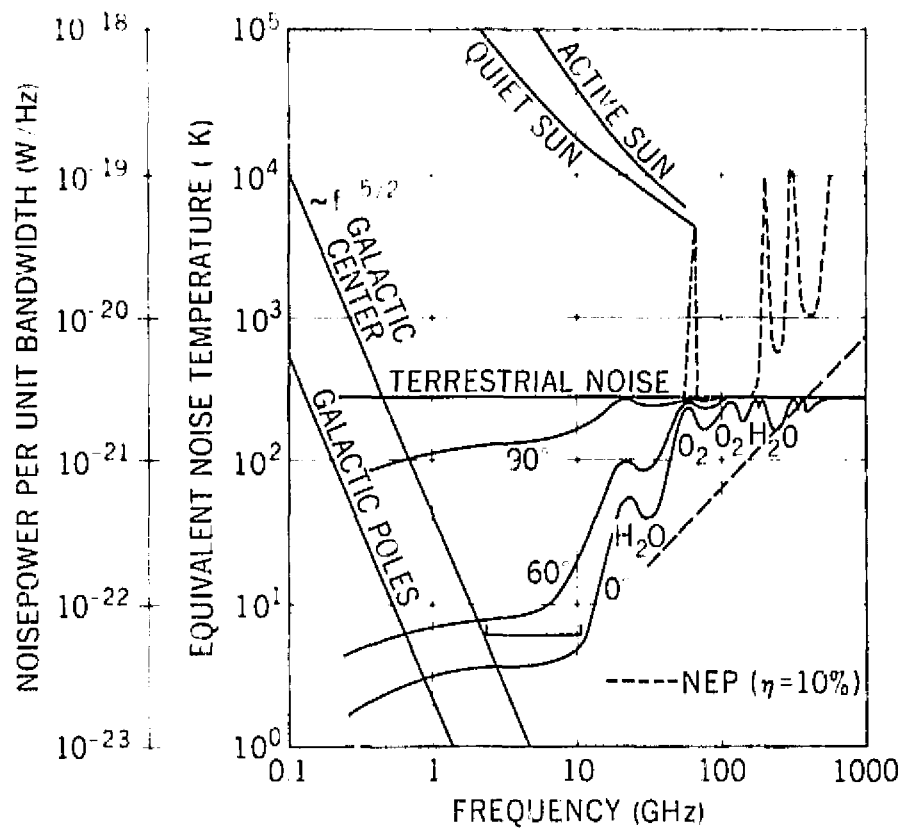


Figure 15—Composite external noise profile.

millimeter wave region, noise related to molecular wave interaction with oxygen and water vapor is predominant. Plots are shown for vertical and low-elevation-angle propagation paths through the atmosphere. A low-noise window exists for vertical wave incidence in the frequency range 2 to 10 GHz. This range is limited toward lower frequencies by increasing galactic noise and toward higher frequencies by atmospheric noise radiation. The straight dashed line shows the equivalent noise power for quantum energy limitation, assuming a 10% detector efficiency. This is (by definition) the minimum signal energy required for a signal to noise ratio (S/N) of 1. Quantum noise is negligible at millimeter wavelengths, whereas at optical frequencies it is the major noise source. The high peaks are due to atmospheric absorption and are applicable to ground-based receivers only. The atomic hydrogen emission line at 1.42 GHz is limited

to this single frequency, and therefore no interference is to be expected. The equivalent noise temperature is much higher than the galactic noise at this frequency; it is of the order of 100°K .

The emission temperature of particles in the atmosphere is a function of absorptivity and reflectivity of the particles and the temperature of the reflected volume. The calculated emission temperature from the earth's surface into space and from the water vapor contribution of the atmosphere is shown in Figure 16. The contribution of O_2 is not included. Emission temperature reversals at center frequencies in the water vapor line are due to the dependence of absorptivity and atmospheric gas temperature on the altitude (Reference 1).

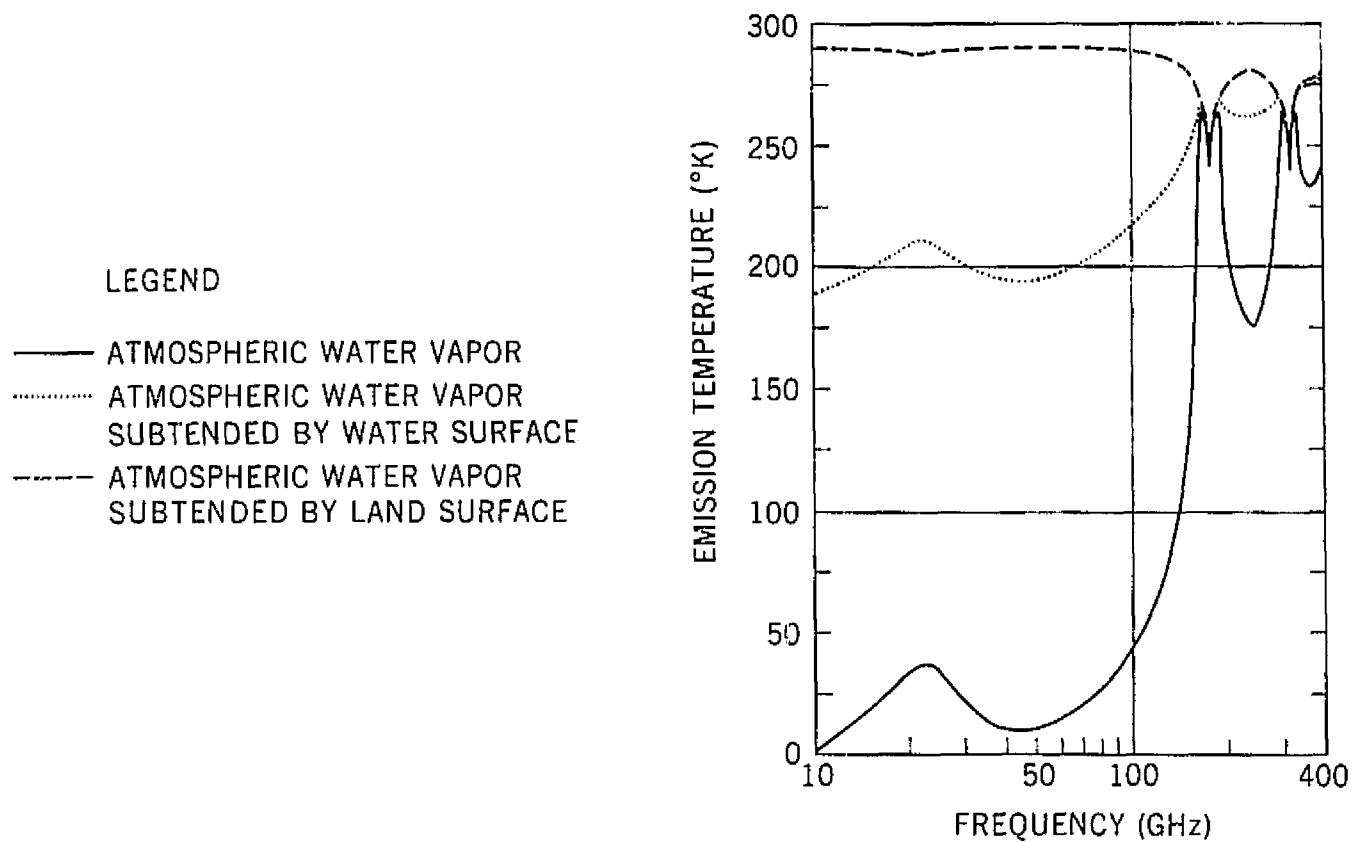


Figure 16—Earth's water vapor emission into space.

Antennas outside the earth's atmosphere directed toward space will have a noise temperature near zero (that is 3°K due to the recently discovered isotropic black-body radiation). Exceptions are those solid angles subtended by sun, moon, and planets of our solar system. Antennas directed toward the earth will have temperatures between 200° and 300°K depending upon the wavelength and the nature of the earth's surface subtending the volume viewed by the antenna.

CHANNEL CHARACTERIZATION

General

The different physical effects have been discussed. A wide variety of signal distortion is introduced by atmospheric gases, rain, and clouds. There is also a great dependence on time and location. These physical mechanisms of wave propagation are of interest to the propagation engineer. Questions like these, however, actually do not offer much guidance to the communication engineer. He is concerned primarily with the overall effects of the transmission channel upon signals. The signals are usually delivered to the channel through a pair of terminals and acquired from it at another pair of terminals. Therefore, a description of the terminal behavior of the channel as a "black box" is the most direct approach to the characterization of the transmission medium. However, although the channel performance may be expressed in terms of black-box parameters, the estimation or prediction of these parameters must fall upon propagation studies, taking into account physical data such as antenna site locations, atmospheric conditions, and so forth.

Many communication channels in use today, and also the millimeter wave channels, are subject not only to additive noise but also to time and frequency spreading. The transmission characteristics of such a channel are specified by a time-varying transfer function. Even if this function could be measured, using it to characterize a given channel would be somewhat akin to using a sample function to describe a random process. In other words, this function contains too much data to be useful without processing. In this discussion, interest extends only to finding various averages of the transfer function.

Black-Box Parameters

The first averages that are of interest are mean and mean-square values which give information about attenuation and scintillation. Of interest also are the statistics of the signal which indicate the usefulness of a theoretical channel model (Rayleigh, Rician, and others). All these averages will change with time, that is with changing atmospheric conditions. Therefore, it is necessary to have time plots and cumulative distributions for each of these parameters.

The importance of the mean value (attenuation) is self-explanatory. It is needed to determine the power budget for a planned communication channel. The S/N ratio and the channel statistics are used to derive the expected error probabilities. As an example, the error probability versus S/N for Rician fading channels is shown in Figure 17. Note the two limiting cases (Rayleigh fading and nonfading). The best performance is achieved on a nonfading channel and the worst performance is on a pure scatter channel. Here the assumption is

made that the channel is neither frequency nor time selective. If selectivity is added, the channel performance becomes worse.

Channel Characterization Function

To describe the selectivity of a fading channel, additional parameters are needed. The different correlation and scattering functions and their relations to each other are shown in Figure 18. *

Time spreading, often called multipath smear or dispersion, manifests itself most clearly when a narrow pulse at the channel input is converted into an output that is spread out over a significant period of time. Frequency spreading, often called Doppler spreading, manifests itself most clearly when a sinusoidal input is converted into an output that is spread over a significant band of frequencies. The distortion of arbitrary waveforms due to these phenomena is more serious for communication purposes than the problems created by additive noise. The degree to which multipath and Doppler spreading harm a communication signal is dependent in part on the character of the signal. A highly redundant signal, such as speech, will be harmed less by the same perturbation than a nonredundant signal, such as coded speech or a data stream.

When the bandwidth of a transmitted signal is small compared to the coherence bandwidth of the fading transmission medium, the received signal differs from the transmitted signal, apart from additive noise, only in having a random

*Final Report for Millimeter Communication Propagation Program Extension, prepared by the Raytheon Co. under NASA contract NAS5-9523, March 1966 to Feb. 1967.

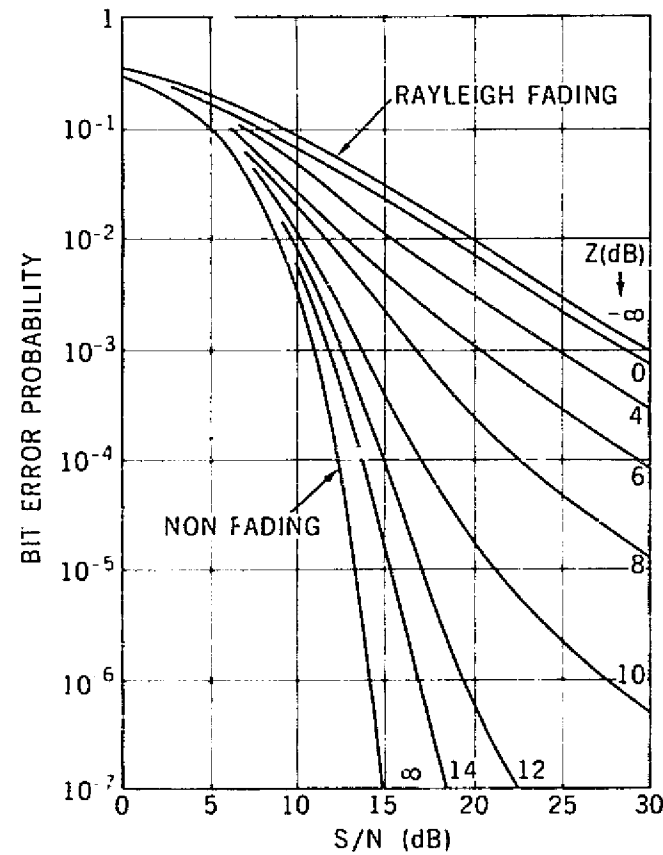


Figure 17—Bit error probability for Rician fading flat-flat channel (order of diversity = 1, noncoherent FSK).

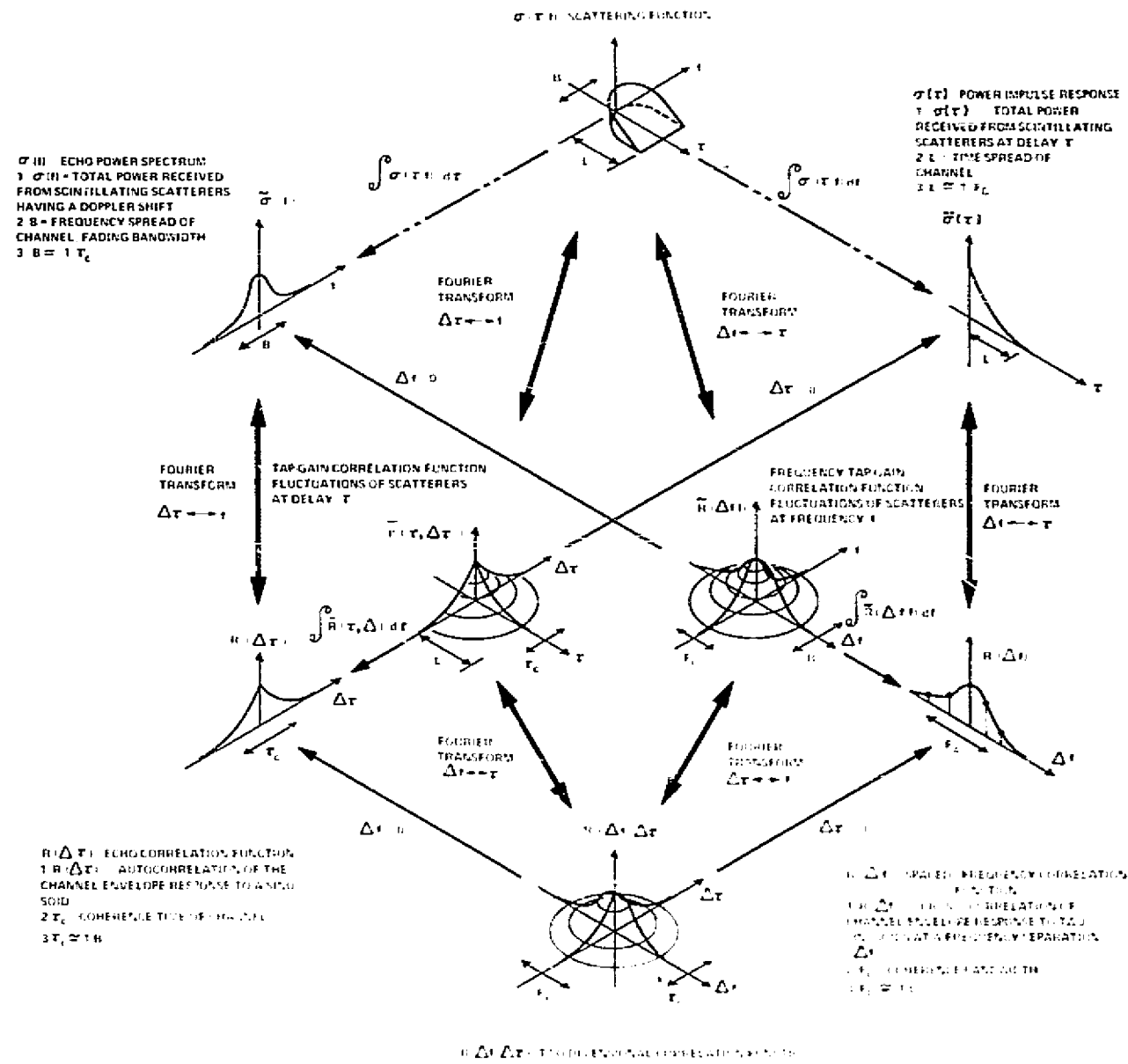


Figure 18—Correlation and scattering functions.

amplitude and phase modulation superimposed. This type of fading is called flat fading, since, in producing the output signal, the channel causes all frequency components of the transmitted signal to suffer the same random amplitude and phase modulation. As the bandwidth of the transmitted signal increases and begins to approach the coherence bandwidth of the channel, a "frequency selective" fading begins to manifest itself; that is, all frequency components in the transmitted signal no longer suffer the same random modulation. The presence of frequency and also time-selective fading is especially harmful in non-linear modulation schemes such as frequency modulation and pulse modulation, since it produces intermodulation components.

How can these rather complicated functions be measured? This can be done through the use of different test signals (References 7 and 8). When a simple sine wave is used, the auto-correlation of the received carrier yields the echo correlation function. Two cuts through the correlation function parallel to the $\Delta\tau - R$ plane were obtained by modulation of the carrier with another sine wave of frequency Δf and calculation of the cross-correlation function of received lower and upper side tone (Figure 18). The two-dimensional correlation function can be constructed with various values of Δf .

In order to measure the complex correlation function (amplitude and phase), one would need very stable frequency sources. Since those are not available at the millimeter wave region, one can only measure the correlation function of the envelopes. There exists a rather complicated relationship between these two correlation functions (Reference 9).

ATTENUATION MEASUREMENTS

From the previous discussion it is clear that the performance of an earth-to-space communication system at millimeter wavelengths is heavily dependent on frequency, atmospheric conditions, and orientation of the spacecraft with respect to the observer. Regions of relatively low attenuation below 100 GHz exist at 15 GHz (not truly millimeter region), 35 GHz, and 94 GHz. Attenuation and noise are lower at 15 and 35 GHz, and equipment is more advanced than at 94 GHz. Long term measurements of atmospheric attenuation, channel parameters, and noise level conducted over a wide variety of meteorological conditions are required in order to obtain the quantitative results needed to estimate the reliability of a communication system.

A number of methods can be used to measure the characteristics of a communication path and to determine the black-box parameters. For point-to-point communications on earth, the experiments are not usually too difficult to conduct, since both transmitter and receiver terminals are located on the ground. For earth-to-space communications the experiments are complicated due to the fact that one of the terminals (or a reflector) must be placed in space, thus requiring the use of an aircraft, rocket, or satellite. A program of this type presents many problems because of the time, cost, and risk involved. It appears that it may be possible to obtain information on propagation through the earth's atmosphere at millimeter wavelengths using a relatively strong radio source, such as the sun. Since incoherent radiation is emitted from the sun, a radiometer is used in place of the conventional coherent signal type receiver.

There are three different types of indirect attenuation measurement:

(1) Sky temperature measurements. This information is very useful in determining the noise contribution of the atmosphere in order to estimate the sensitivity to be expected in a low-noise system. To calculate attenuation from the measured sky temperature, the atmospheric model has to be known (or assumed). The extent to which atmospheric sky temperature and attenuation are correlated can only be determined by making simultaneous measurements over a long period of time.

(2) Suntracker. Use of the sun as a source of millimeter wave radiation has one major disadvantage. Since the sun moves continuously, relative to the earth, only a short time is spent looking in a given direction. The applicability of the secant law is very risky. Amplitude and fading rate of the scintillations cannot be measured using the sun, since it is a relatively large source and the fluctuations will average out. Scintillations are produced by blobs which are small compared to the solid angle of the sun.

Measured attenuation at 35 GHz as a function of zenith angle under various meteorological conditions (Reference 10) is illustrated in Figure 17. The values T_g and ρ refer to the average surface temperature and absolute humidity during the measurement period. The two lowest curves are typical for warm, humid days and for cold, dry days under conditions of clear sky. Attenuation on clear summer days is caused principally by water vapor, and since there are wide fluctuations in absolute humidity, considerable variations in day-to-day

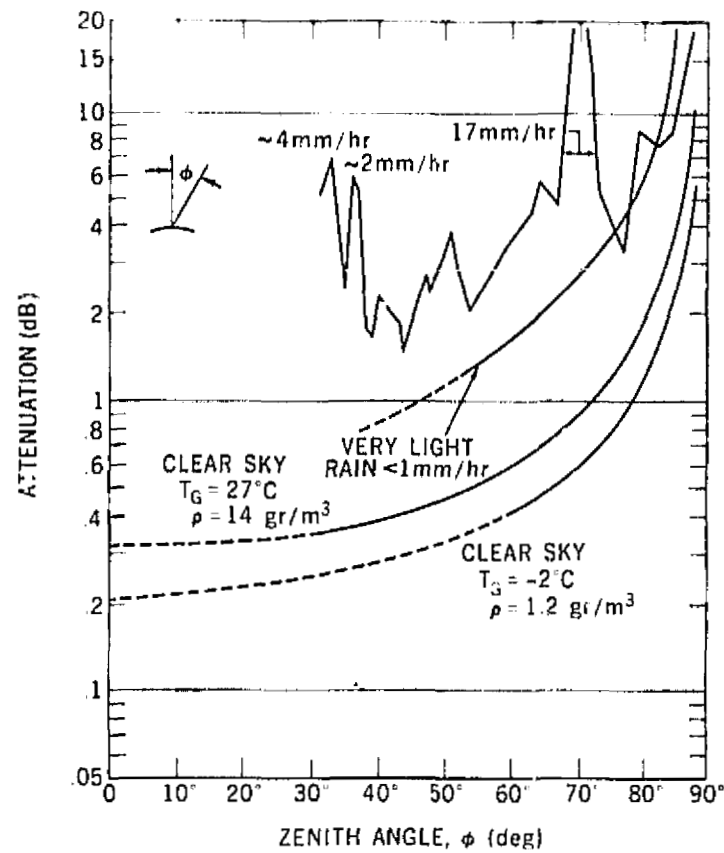


Figure 19—Measured total atmospheric attenuation at 35 GHz (Wulfsberg).

attenuations can be observed. This is in contrast to winter days, when the water vapor content is so low that oxygen absorption becomes predominant and clear sky attenuation is quite stable with time. The upper curve indicates the large and rapid variations in attenuation as a result of variable cloud cover and rain. The lower curves follow the secant law reasonably well. Yet, the upper curve shows clearly that an extrapolation from one elevation angle to another is impossible during cloudy conditions and rain. This is a considerable drawback in the use of suntracker measurements for reliability estimates of a communication link.

(3) Radar. Radar measurements used for calculating the attenuation are not promising since the radar return signal is proportional to the sixth power of

the diameter of the rain drops, but the attenuation is roughly proportional to the third power of the diameter. Also, radar responds to ice particles, which do not play a significant role in attenuation.

Calculation of attenuation from rainfall rate and drop-size distribution does not yield sufficiently accurate results even for a ground link. For an earth-to-space link one has to expect even worse results since rainfall rate, drop-size distribution, and even the path length influenced by rain are not known and ground data are not sufficient to determine the attenuation on a slant path.

Only limited information can be obtained through radiometric and radar measurements, and true system performance, particularly bandwidth information, can only be obtained with a coherent signal. That means that a satellite must be used as a terminal. A beacon in synchronous orbit would be an ideal source for propagation experiments. The tests would allow determination of the feasibility of the link, since attenuation, signal-to-noise ratio, fade rate, fade amplitude, and bandwidth limitations could all be measured as functions of atmospheric conditions and elevation angles (that is, for various ground stations).

The first millimeter wave propagation experiment is onboard the ATS 5 spacecraft. The objective of this experiment is to determine statistically the propagation parameter, which was discussed earlier. *

*Binkley, W. O., et al., "The ATS-E Millimeter Wave Propagation Experiment," NASA/GSFC X-733-68-196, April 1968.

Improvement by Path Diversity

Rain is the most serious problem for millimeter wave communication but fortunately the rain cells are limited and rather small in time and space.

Therefore, the reliability of a system can be improved with some kind of a path-diversity technique. If there are n independent stations, each of which has reliability p , then the overall reliability is given by

$$P = 1 - (1 - p)^n.$$

Station reliability required to achieve system reliabilities of 95%, 99%, 99.9%, and 99.99% is given in Table 2. For example, three stations that are usable 78% of the time would result in a system that is usable 99% of the time. This oversimplified argument (which unfortunately is frequently used) suffers from two major deficiencies. Independent statistics are assumed at the different receiving sites, whereas high-altitude cloud cover and weather patterns tend to be correlated over certain areas. Also, the argument discusses the probability of having at least one station operating at a given time. It does not discuss the time statistics of the resulting outages. Information on outage statistics is required before any meaningful system-design work can be done.

Table 2—Station reliability required for n stations to give system reliability of 95% to 99.99%

Number of Stations	System Reliability			
	95%	99%	99.9%	99.99%
n	95%	99%	99.9%	99.99%
1	95%	99%	99.9%	99.99%
2	78%	90%	96.8%	99.00%
3	63%	78%	90.0%	95.36%
4	53%	68%	82.2%	90.00%

The increase in reliability on a switched-path diversity system has been evaluated from a 4-year period of rainfall data taken at the Bedford network (Reference 11). The paths considered were both 3-km long; they were parallel to each other and separated by a distance of 2 km. The distribution of attenuation for this switched-path case is plotted, along with distribution of attenuation for the case of a single path (Figure 20). With the 30-dB level as a reference value, it is seen that the reliability is improved by a factor of 10 through use of path diversity (outage time is reduced from 10 minutes to 1 minute per year). On the other hand, with a reliability factor of 10 min/year per link (about 0.002

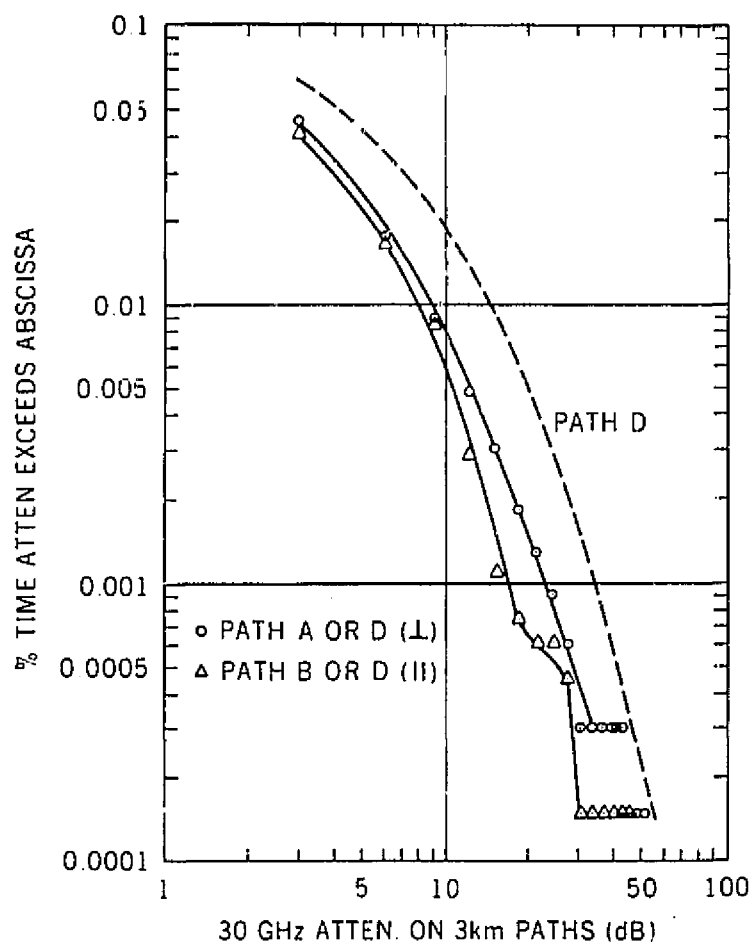


Figure 20—Distributions for switched diversity on orthogonal paths (A or D) and on parallel paths separated by 2 km (B or D) compared with that of a single path.

on the percentage of time scale), the effective attenuation is only 14 dB for the diversity distribution, as compared with 28 dB for the single path. Thus, longer path lengths may be used in the diversity system.

Much more extensive and complete data on space diversity will be needed before such installation can be designed with confidence. The optimum spacing for a given performance probability can only be obtained from experiments.

REFERENCES

1. Tolbert, C.W., and Straiton, A.W., "Synopsis of Attenuation and Emission Investigations of 58 to 62 kMc Frequencies in the Earth's Atmosphere." Proc. IEEE 51:1754-1760, December 1963.
2. Hogg, D.C., "Millimeter-Wave Communication Through the Atmosphere." Science 159:39-46, January 1968.
3. Rosenblum, E.S., "Atmospheric Absorption of 10-400 kMeps Radiation: Summary and Bibliography to 1961." Microwave J. 4(3):91-96, March 1961.
4. Meeks, M.L., and Lilley, A.E., "The Microwave Spectrum of Oxygen in the Earth's Atmosphere." J. Geophys. Res. 68(6):1683-1703, March 1963.
5. Medhurst, R.G., "Rainfall Attenuation of Centimeter Waves: Comparison of Theory and Measurement." IEEE Trans. Antennas Propagat. 13:550-564, July 1965.
6. Bussey, H.E., "Microwave Attenuation Statistics Estimated From Rainfall and Water Vapor Statistics." Proc. IRE 38:781-785, July 1950.
7. Gallager, R.G., "Characterization and Measurement of Time- and Frequency-Spread Channels," Lincoln Laboratory, Mass. Inst. Technol., Technical Report 352, April 1964.
8. Bello, P.A., "Measurement of the Complex Time-Frequency Channel Correlation Function," J. Res. Nat. Bur. Stand., Sect. D, Radio Sci. 68D(10):1161-1165, October 1964.
9. Mondre, E., "Relationship Between Complex and Envelope Covariance for Rician Fading Communication Channels," NASA Technical Note D-4825.
10. Wulfsberg, K.N., "Sky Noise Measurement at Millimeter Wavelengths." Proc. IEEE 52:321-322, March 1964.
11. Hogg, D.C., "Path Diversity in Propagation of Millimeter Waves Through Rain." IEEE Trans. Antennas Propagat. 15:410-415, May 1967.